

Modelling acoustic scattering, sound speed, and attenuation in gassy soft marine sediments

A. Mantouka, H. Dogan, P. R. White, and T. G. Leighton^{a)}

Institute of Sound and Vibration Research, Faculty of Engineering and the Environment, University of Southampton, Highfield, Southampton SO17 1BJ, United Kingdom

(Received 30 April 2015; revised 18 April 2016; accepted 9 June 2016; published online 14 July 2016)

A model for nonlinear gas bubble pulsation in marine sediments is presented. This model is then linearized to determine the resonance frequency and the damping terms for linear radial oscillations. The linear model is then used to predict the effects that such bubble pulsations will have on the sound speed and attenuation of acoustic waves propagating in gassy marine sediment. The results are compared for monodisperse populations against the predictions of a model of Anderson and Hampton and, furthermore, the additional abilities of the model introduced in this paper are discussed. These features include the removal of the sign ambiguities in the expressions, the straightforward implementation for acoustic propagation through polydisperse bubble populations, the capability to estimate bubble size distributions through a full acoustic inversion, and the capability to predict nonlinear effects.

© 2016 Acoustical Society of America. [<http://dx.doi.org/10.1121/1.4954753>]

[NPC]

Pages: 274–282

NOMENCLATURE

A	attenuation in gassy sediment
c_p	speed of sound in host medium
c_{pb}	complex sound speed in gassy sediment
D_g	thermal diffusivity of gas
G^*	complex sediment shear modulus
G_m	solid matrix shear modulus
G_s	real part of complex sediment shear modulus
G_s'	imaginary part of complex sediment shear modulus
G_w	water shear modulus
f	frequency
i	imaginary unit number
I_0	incoming acoustic intensity
I_s	scattered acoustic intensity
K_g	thermal conductivity of gas
K_m	solid matrix bulk modulus
K_s	sediment bulk modulus
K_w	water bulk modulus
m_{eff}	effective bubble mass
n_b	bubble number density
p	an attenuation exponent
p_0	hydrostatic pressure
p_g	gas pressure inside the bubble
p_v	vapor pressure inside the bubble
$p_{\sigma,0}$	Laplace pressure when the bubble is at equilibrium radius
P_A	amplitude of acoustic driving pressure
P_b	pressure radiated from a bubble
r	spatial coordinate
R	bubble radius
R_0	equilibrium bubble radius
\dot{R}	bubble wall velocity
\ddot{R}	bubble wall acceleration
x	normalized bubble wall displacement

t	time
S_v	volume backscattering strength
V	phase velocity

Greek

α	attenuation in water saturated sediment
β	dimensional damping coefficients
γ	gas polytropic exponent (adiabatic)
ε	strain
$\dot{\varepsilon}$	strain rate
Γ	constant in an empirical relation
η_s	sediment shear viscosity
η_{th}	thermal viscosity
η_w	viscosity of water
κ	gas polytropic exponent
ζ	porosity
ρ_G	density of the gas inside the bubble
ρ_m	density of the mineral grains
ρ_s	density of water-saturated sediment
ρ_w	density of the seawater
σ	surface tension
σ_s	scattering cross-section
σ_v	scattering cross-section for a bubble distribution
$\sigma_{v,\text{ref}}$	reference volume cross-section
τ	stress tensor
Φ	complex polytropic exponent
χ	thermal diffusion length
ω	angular frequency
ω_0	bubble resonance frequency

I. INTRODUCTION

Characterisation of the amount of gas in marine sediment is important for several reasons. First, for understanding the stability of the sediment with respect to both natural disturbances, such as undersea landslip, and manmade

^{a)}Electronic mail: T.G.Leighton@soton.ac.uk

processes, such as piling for civil engineering projects.^{1–3} Second, for assessment of the gas reserves for fuel and climate risk.^{4–7} Such quantification of marine gas reserves should also take into account that which could potentially dissociate from hydrate. Third, for monitoring leakages into sediment from buried manmade gas bodies, including buried gas pipelines and carbon capture and storage facilities.^{4,8–10} Fourth, the resonance of gas bubbles in sediment can profoundly perturb the propagation and scattering of acoustic waves. Accurate models of these effects are needed to predict the performance of the systems that might, *in situ*, involve propagating waves through gassy sediments (e.g., for sending data to and from buried transponders, for sub-bottom surveying¹¹ and for *in situ* calibration¹²). Accurate models are also needed if the measured attenuation and sound speed are to be inverted to estimate the gas bubble population present in the sediment. The current models for bubble dynamics in sediments are insufficient for inverting measured acoustical propagation and scattering in order to estimate the bubble populations present in the seabed, unless very specific conditions are assumed (e.g., all bubbles are much smaller than the bubble size that resonates with the sound field¹¹). Furthermore, since the attenuation can be high, the source levels used (to provide an adequate signal-to-noise ratio at the receiver) might generate nonlinear bubble oscillations for part of the propagation path, and indeed some methods for measuring or exploiting sub-bottom bubbles might rely on such nonlinearities.^{13–18} Consequently, the inclusion of bubble nonlinearities into such models could, at times, be important.^{19,20}

Acoustic propagation in marine sediments has been extensively investigated. The forward models mainly fall into the following categories: A large body of literature assumed the existence of one compressional and one shear wave, and explored ways to model the frequency dependence of attenuation, α (dB/m), with the following empirical relation:²¹

$$\alpha = \Gamma f^p, \quad (1)$$

where p is the attenuation exponent, f is the frequency and Γ is a constant. There is a broad range of reported values covering a variety of marine sediments^{22–34} although the reported values of p are not consistent between experiments, most probably because of the different sediment types and frequency ranges considered. The value of p is frequently reported as representing a linear model of attenuation (e.g., Wood and Weston³⁵ and Bowles³⁶). However, there are also a number of studies that report attenuation exponents which exhibit nonlinear attenuation relationships (e.g., Stoll,³⁷ Brunson and Johnson,³⁸ and Turgut and Yamamoto³³).

In water-saturated sediment, Biot^{39,40} showed the existence of two compressional waves and one shear wave; this has been consistently validated through experimental work.^{37,41,42} Although Biot's work initially suggested negligible dispersion of compressional waves, later studies have reported significant dispersion in a wide range of excitation frequencies, i.e., 1–100 kHz (Ref. 43) or 10 kHz–1 MHz (Ref. 44). The majority of the studies which aimed to model

the inclusion of gas bubbles into porous sediment have assumed that the bubbles are contained only in the pore fluid spaces and they do not affect the sediment structure.^{45–47} This assumption implies that the contact between the gas bubble and the sediment mineral grains is not taken into account; hence, those models are not applicable to the “sediment-replacing” type of bubble in the classification of Anderson *et al.*⁴⁸ To our knowledge, the work of Kargl *et al.*⁴⁹ is the only publication that takes into account the effects of sediment rigidity on the pulsations of bubbles and the presence of two compressional waves, and investigates the double resonance behaviour of bubbles under the effect of two compressional waves. However, their model leaves out the formulation of damping, sound speed and attenuation relevant to bubble pulsations and does not provide a route for acoustic inversion. The notable contribution of Boyle and Chotiros^{50,51} also formulated the propagation of two compressional waves in sediment containing gas bubbles, although the viscoelastic damping was attributed to the pore water viscosity only, which may result in underestimation of the attenuation caused by bubbles.

Anderson and Hampton^{52,53} presented the model that is most frequently used for predictions of acoustic scattering, sound speed and attenuation in gas-bearing marine sediments. The applicability of this model is limited to linear gas bubble pulsations, and leaves ambiguities for the inverse problem because of the plus/minus sign entering the expression of the complex sound speed [Eq. (49) of Ref. 52]. This sign ambiguity may result in the presence of both positive and negative bubble counts when inverting broadband acoustic data. For instance, Best *et al.*⁵⁴ measured the attenuation spectra between 600 and 3000 Hz and identified five peaks which were attributed to bubble resonances. The attenuations for these single bubble sizes were computed theoretically [their Figs. 9(a) and 9(b)] in order to obtain the bubble number density, which were then weighted to estimate a continuous bubble size distribution (their Fig. 10). However, the weightings with best fit to the measured attenuation gave a poor fit to the sound speed data [their Fig. 9(c) and 9(d)]. The method outlined in this paper, on the other hand, is suitable for a full acoustic inversion which satisfies both sound speed and attenuation data simultaneously.⁵⁵

Lyons *et al.*⁵⁶ have also performed predictions of bubble populations in gassy sediment using the linear scattering cross section expressions [Eqs. (54)–(56)] of Anderson and Hampton (equations that are not self-consistent^{57,58}). The model presented in Sec. II is suitable for implementation with short high amplitude pulses (as required for range resolution⁵⁹), and for nonlinear inversions, e.g., when the high amplitudes required to overcome sediment attenuation produce harmonics, ultraharmonics, and subharmonics in the bubble wall displacements⁵⁵ or produce nonlinear mixing of two insonification frequencies,^{60–62} a technique which is receiving increasing interest in sediment studies.^{16–18,63,64}

In this work, it is assumed that the gas-free host medium supports one compressional and one shear wave. Furthermore, the dispersion of the first compressional wave and the dissipation due to internal friction are neglected. Whilst more comprehensive studies should address mismatches between such

assumptions and observations, such an exercise is beyond the scope of this article, which restricts itself to the regime of assumptions about dispersion that were used in the model of Anderson and Hampton, against which the predictions of the new model are compared. Incorporation of the second compressional wave and the other losses into the model requires a more comprehensive treatise, i.e., by expanding the formulation of Kargl *et al.*⁴⁹ to a nonlinear setting. However, this is not a straightforward task since the Biot theory itself is inherently linear. The effective bulk and shear moduli of the host medium, on the other hand, are calculated in this work using a comprehensive model based on Berryman's self-consistent approximation.^{65,66}

II. BUBBLE DYNAMICS

Leighton²⁰ presented a nonlinear time-dependent model for bubble dynamics in a viscoelastic medium, i.e., marine sediments. It incorporated the shear properties of the host medium, and that paper identified that the next stage in developing that formulation would be to replace the assumption of an incompressible host medium with one that includes acoustic radiation losses. This is the objective of the current paper, which combines the general form of the Keller–Miksis equation with the linear Voigt viscoelastic model.

Consider the radial motion of a spherical gas bubble of radius $R(t)$ which is fixed in space and oscillates about some equilibrium radius R_0 with bubble wall velocity $\dot{R}(t)$. Assuming the flow is irrotational (implying that the porosity is a homogenous property of the host medium) yields the following equation for radial bubble dynamics which accounts for the compressibility of the surrounding medium to first order.⁶⁷

$$\begin{aligned} & \rho_s \left(1 - \frac{\dot{R}}{c_p} \right) R \ddot{R} + \frac{3}{2} \rho_s \left(1 - \frac{\dot{R}}{3c_p} \right) \dot{R}^2 \\ & = \left(1 + \frac{\dot{R}}{c_p} + \frac{R}{c_p} \frac{d}{dt} \right) \left(p_g - \frac{2\sigma}{R} - p_0 + P_{AG}(t) \right. \\ & \quad \left. - \frac{4\eta_s \dot{R}}{R} - \frac{4G_s}{3R^3} (R^3 - R_0^3) \right). \end{aligned} \quad (2)$$

Equation (2) was first proposed by Yang and Church²⁷ in order to model the acoustic propagation in viscoelastic tissues; it is also applicable to marine sediments provided that the appropriate viscoelastic constitutive relation is employed. It includes the acoustic radiation losses; several routes for the incorporation of such losses into a Rayleigh–Plesset-type equation were outlined in Ref. 20.

In Eq. (2), G_s is the shear modulus, η_s denotes the shear viscosity, p_0 is the static pressure outside the bubble, p_g is the pressure within the bubble, and σ denotes the surface tension at the bubble wall. The equilibrium gas pressure p_{g_0} can be expressed in terms of p_0 , the Laplace pressure when the bubble is at equilibrium radius ($p_{\sigma,0} = 2\sigma/R_0$) and vapour pressure p_v as:

$$p_{g_0} = p_0 + \frac{2\sigma}{R_0} - p_v. \quad (3)$$

The compressional sound speed c_p and the density ρ_s refer to that of water-saturated sediment which surrounds the gas bubble and can be obtained from

$$c_p = \sqrt{\frac{K_s + 4G_s/3}{\rho_s}} \quad (4)$$

and

$$\rho_s = \xi \rho_w + (1 - \xi) \rho_m, \quad (5)$$

respectively, where K_s is the bulk modulus of the water-saturated sediment, ξ is the porosity, ρ_w is the water density, and ρ_m the grain mineral density.

Berryman^{65,66} suggested a self-consistent method to calculate the effective bulk modulus of a composite medium, which states (as applied to the present problem)

$$\frac{1}{K_s + 4G_s/3} = \frac{1 - \xi}{K_m + 4G_s/3} + \frac{\xi}{K_w + 4G_s/3}, \quad (6)$$

$$\frac{1}{G_s + F} = \frac{1 - \xi}{G_m + F} + \frac{\xi}{G_w + F}, \quad (7)$$

where

$$F = \left(\frac{G_s}{6} \right) \frac{9K_s + 8G_s}{K_s + 2G_s}. \quad (8)$$

In Eqs. (6) and (7), K_m refers to the bulk modulus of the solid matrix, K_w is the bulk modulus of pore water, G_m is the shear modulus of the solid matrix, and G_w denotes the shear modulus of pore water which is related to the shear viscosity of water with $G_w = i\omega\eta_w$.

A. Thermal losses

The Yang and Church model formulated the thermal processes within the bubble assuming an ideal gas with polytropic index κ :

$$p_g = p_{g_0} \left(\frac{R_0}{R} \right)^{3\kappa}. \quad (9)$$

If the value of κ is constant throughout the bubble pulsation, the heat transfer across the bubble wall is reversible, and the above model does not predict any irreversible heat transfer (Leighton *et al.*⁵⁵).

Prosperetti *et al.*⁶⁸ used nonlinear energy conservation to provide a formulation for the thermal losses during the expansion and compression of a spherical gas bubble. It was shown that, in the linear limit, these irreversible heat losses can be modelled with

$$p_g = p_{g_0} \left(\frac{R_0}{R} \right)^{3\kappa(\omega)} - 4\eta_{th} \frac{\dot{R}}{R}, \quad (10)$$

where $\eta_{th} = (3p_{g_0}/4\omega) \text{Im}(\Phi)$ is the ‘‘thermal viscosity’’ and ω is the angular frequency. According to Prosperetti *et al.*,⁶⁸ the effective polytropic index $\kappa(\omega)$ is

$$\kappa(\omega) = \frac{1}{3} \text{Re}(\Phi), \quad (11)$$

where the complex function

$$\Phi = \frac{3\gamma}{1 - 3(\gamma - 1)i\chi \left[\left(\frac{i}{\chi}\right)^{1/2} \coth\left(\frac{i}{\chi}\right)^{1/2} - 1 \right]}, \quad (12)$$

depends on the adiabatic polytropic exponent γ and the thermal diffusivity of the gas D_g through the thermal diffusion length

$$\chi = \frac{D_g}{\omega R_0^2}. \quad (13)$$

Although the use of a thermal viscosity to capture thermal losses remains approximate (there remains, for example, discussion as to the choice of frequency for use in the formulation when the bubble pulsation is not monochromatic), it gives a usefully simply analytical tool that avoids the complexities of calculating thermal losses from, say, maps of the time-dependent bubble volume response as a function of driving pressure.⁵⁵

B. Viscoelastic constitutive relation

The Voigt constitutive model used in the bubble dynamics model Eq. (2) can be expressed as

$$\tau = G_s \varepsilon + \eta_s \dot{\varepsilon}, \quad (14)$$

where ε is the strain and $\dot{\varepsilon}$ is the strain rate. The Voigt model is appropriate for most marine sediments since the acoustic excitations induce small strains.^{20,69,70} This model indicates that the total stress field in the medium will produce a superposition of both elastic and viscous responses (see schematic inset into Fig. 1). The common approach in terms of modeling the viscoelastic behaviour of marine sediments has been to treat the medium as a lossy elastic solid by using a complex shear modulus:^{71,72}

$$G^* = G_s + i G'_s. \quad (15)$$

The shear viscosity of the sediment is then deduced from the imaginary part of the shear modulus (equivalently from shear wave attenuation):^{53,54,70,73}

$$\eta_s = \frac{G'_s}{2\pi f}. \quad (16)$$

III. LINEARIZATION

To address the linear bubble dynamics problem, the resonance frequency and the linear damping terms will be derived from Eq. (2). Solutions to the linear problem can be found by assuming small amplitude pulsations $x \ll 1$ about the bubble equilibrium radius R_0 , i.e., $R = R_0(1 + x)$. Grouping the terms x , \dot{x} , and \ddot{x} generates the following linearized formulation:

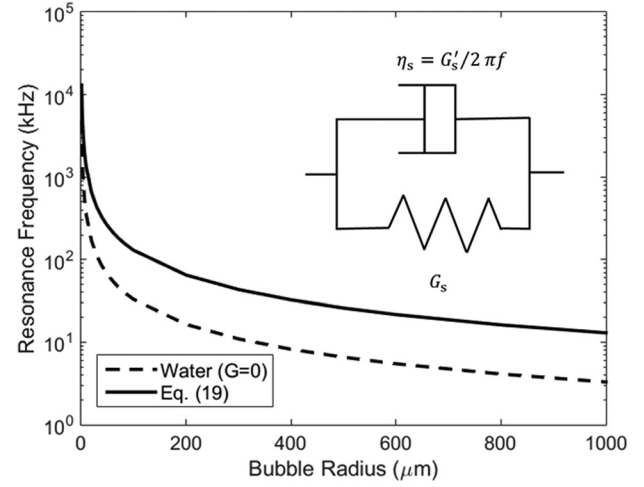


FIG. 1. Bubble resonance frequency vs bubble size (R_0). The solid line is calculated by Eq. (19) and the dashed line is calculated from the same equation by setting the shear modulus to zero. The input parameters for both cases are shown in Table I. The inset shows a schematic of a mechanical spring-dashpot analogue representing the responses of a rheological elementary model: the Voigt model with constant parameters. The shear viscosity for sediments is deduced from the imaginary part of the shear modulus, i.e., $\eta_s = G'_s/2\pi f$.

$$\ddot{x} + 2\beta_{\text{tot}}\dot{x} + \omega_0^2 x = -\frac{P_A e^{i\omega t}}{m_{\text{eff}}}, \quad (17)$$

where m_{eff} is the effective mass

$$m_{\text{eff}} = \rho_s R_0^2 + \frac{4\eta_s R_0}{c_p}. \quad (18)$$

The terms in Eq. (17) include the resonance frequency for the bubble wall displacement

$$\omega_0^2 = \left(3p_{g_0} \text{Re}(\phi) - \frac{2\sigma}{R_0} + 4G_s \right) / \left(\rho_s R_0^2 + \frac{4\eta_s R_0}{c_p} \right), \quad (19)$$

and the term β_{tot} , which has units of (1/s) and is sum of the following five damping terms, namely, the radiation, the viscous, the thermal, the interfacial and the elastic:

$$\beta_{\text{vis}} = 2\eta_s / \left(\rho_s R_0^2 + \frac{4\eta_s R_0}{c_p} \right), \quad (20a)$$

$$\beta_{\text{p-th}} = \left(\frac{3p_{g_0} \text{Im}(\phi)}{2\omega} \right) / \left(\rho_s R_0^2 + \frac{4\eta_s R_0}{c_p} \right), \quad (20b)$$

$$\beta_{\text{rad}} = \frac{\rho_s \omega^2 R_0^3}{2c_p} / \left(\rho_s R_0^2 + \frac{4\eta_s R_0}{c_p} \right), \quad (20c)$$

$$\beta_{\text{int}} = -\sigma / (\rho_s c_p R_0^2 + 4\eta_s R_0), \quad (20d)$$

$$\beta_{\text{el}} = 2G_s / (\rho_s c_p R_0 + 4\eta_s), \quad (20e)$$

where

$$\beta_{\text{tot}} = \beta_{\text{vis}} + \beta_{\text{p-th}} + \beta_{\text{ac}} + \beta_{\text{int}} + \beta_{\text{el}}. \quad (20f)$$

Note the features that differentiate the model established here from the one as applied to soft tissue by Yang and

Church⁶⁷ are (a) the interpretation of the viscoelastic model representing the bubble surrounding medium (i.e., the model parameters G_s and η_s), (b) the interpretation of the parameters that are related to the host medium such as density and sound speed, and (c) the more comprehensive thermal damping which accounts for net heat losses.

A. Sound speed and attenuation

The complex sound speed in sediment containing gas bubbles can be derived from the linearized equation of bubble pulsations following the method outlined by Commander and Prosperetti.⁷⁴ Applicable to the problem considered here, the complex speed of sound in a gassy sediment, c_{pb} , is expressed as

$$\frac{c_p^2}{c_{pb}^2} = 1 + 4\pi c_p^2 \int_0^\infty \frac{R_0 n(R_0)}{\omega_0^2 - \omega^2 + 2i\beta_{tot}\omega} dR_0, \quad (21)$$

where $n(R_0)dR_0$ is the number of bubbles per unit volume with radii between R_0 and $R_0 + dR_0$. Note that β_{tot} includes the elastic damping and the interfacial damping in addition to the other damping mechanisms for bubbles in water. Setting $c_p/c_{pb} = u - iv$ yields the expressions for phase velocity V (Ref. 74)

$$V = c_p/u, \quad (22)$$

and attenuation A in dB/m

$$A = 8.6859 (\omega v/c_p). \quad (23)$$

IV. APPLICATION OF THE MODEL TO GASSY SEDIMENTS

In this section, the model established in Secs. II and III will be applied to gassy sediments by defining appropriate model input parameters. In shallow marine sediments, the gases that are most likely to be encountered are: oxygen (O_2), carbon dioxide (CO_2), nitrogen (N_2), ammonia (NH_3), hydrogen sulphide (H_2S), and methane (CH_4). Their production is mainly controlled by biogeochemical processes associated with the bacterial remineralisation of labile organic matter.⁷⁵ Although in the top sediment layer more than one gas may exist, the dominant ones are oxygen and aerobic respiration products in the aerobic zone, sulphate (and sulphur compounds) in the sulphate-reducing zone and methane in the carbonate reducing zone. Nitrogen is not a major gas in these zones; hence, O_2 is assumed to be the predominant gas.

The density of pore water of seafloor sediments is nearly constant in marine environments and takes values between 1000 and 1030 $kg\ m^{-3}$ (Ref. 41). The mineral density depends on the sediment type. Sands typically comprise quartz minerals with density equal to 2650 $kg\ m^{-3}$, whereas muds are comprised of various minerals (kaolinite, illite, etc.) having densities from 2600 to 2800 $kg\ m^{-3}$ (Mavko *et al.*⁷⁶). In marine sediments, the porosity varies between 0.35 and 0.90 and is generally inversely proportional to the mean grain size.²⁷

The model values in line with these considerations are given in Table I. The value of the surface tension is difficult to determine and not available in literature; it is assumed to take the value for a bubble in salty water (no allowance being made for the level of dirtiness in seawater).

The bubble linear frequency is dominated by the shear modulus. In Fig. 1, the bubble resonance frequency is plotted against the bubble size using Eq. (19) (solid line), where it is shown that it varies with the square root of the shear modulus. On the same figure, the resonance frequency for the same bubble sizes in water (dotted line) is plotted for comparison.

Next, the results for the damping terms are presented in Fig. 2. The results indicate that the acoustic radiation damping is the dominant loss mechanism at high frequencies, justifying the extension suggested in Ref. 20 to include these. An equally important loss mechanism appears to be the viscous damping as formulated by Eq. (20a). The elastic damping, which was not identified in the Anderson and Hampton theory but is formulated here owing to the complete form of the Voigt constitutive model used, is also a significant damping mechanism as can be seen. The effects of the thermal damping are relatively less pronounced and the interfacial damping can be regarded as negligible. However, we should remark that the thermal damping may be a dominant loss mechanism at medium frequencies (according to the range in the figure) depending on the sediment type investigated and the gas content of the medium (e.g., in muddy sediments where rigidity values are much lower and the sediment resembles more fluid-like behaviour). Note that the thermal damping based on the formulation of Prosperetti *et al.*⁶⁸ (labelled as P-thermal) shows qualitatively different behaviour as the frequency changes. The thermal damping according to ideal gas law Eq. (9) does not show frequency dependent behaviour and does not predict any net thermal losses over a cycle if the polytropic exponent is taken as constant.⁵⁵ Overall, the damping characteristics stemming from the elastic properties of the host medium are very significant, indicating that models which have treated the host sediment as water will underestimate the damping.

Using Eqs. (22) and (23), the sound speed and attenuation of an acoustic wave has been computed for monodisperse bubble populations of radii 80, 120, 160, and 200 μm , assuming the input parameters of Table I. The results are shown in Fig. 3 (solid line). On the same figure the sound speed and attenuation are plotted (dotted line) using Eqs.

TABLE I. Model input parameters.

Property	Value	Property	Value
Water depth	1 m	K_m	5×10^{10} Pa
Sediment depth	1 m	G_m	1.2×10^7 Pa
p_0	101325 Pa	G'_s	0.16 MPa
ρ_w	998 kg/m^3	κ	1.4
ρ_s	1640 kg/m^3	σ	0.036 N/m
c_p	1465 m/s	ρ_g	1.202 kg/m^3
K_w	2.3 GPa	K_g	0.0241 W/mK
η_w	0.0018 Pa s	C_{pg}	1001.73 J/kgK
ζ	0.68	D_g	1.9×10^{-5} m^2/s

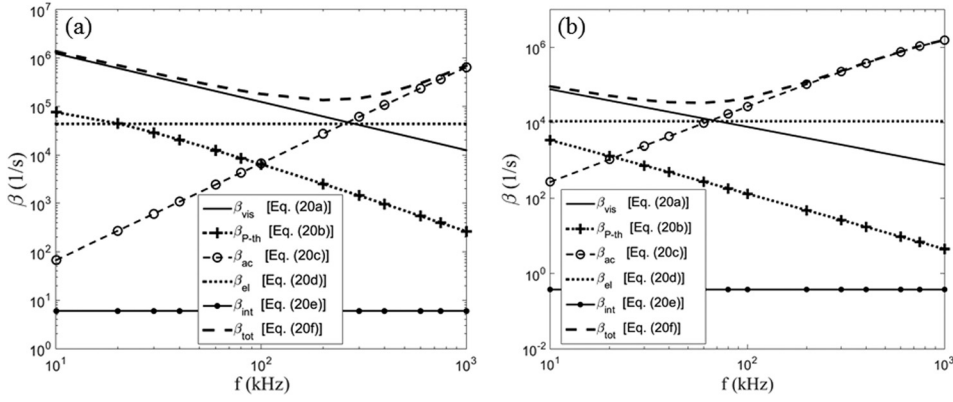


FIG. 2. Dimensional damping constants vs frequency for a bubble with equilibrium radius (a) 50 μm and (b) 200 μm for the parameters listed in Table I.

(49) and (53) of the Anderson and Hampton model.⁵³ The difference in the predictions of these two models is attributed to the differences in the damping terms and the linearization of the fundamental equation used [Eq. (2)]. The results point out similarities at low frequencies and at high frequencies: in the former case, the propagation velocities in the medium is largely determined by the gas void fraction and the bulk modulus of the gas, and in the latter case the sound speed converges to that of water saturated medium. The near resonance regime behaviour of the models, on the other hand, is significantly different. Given that each line in Fig. 3 represents data from a single bubble size, it is anticipated that the discrepancies over a wide frequency range will be significant when attempts are made to model/invert acoustic data from a bubble size distribution. As already discussed, the main

advantage of Eq. (22) is that it does not contain sign ambiguity and it can be used in an inversion model which requires simultaneous information on both sound speed and attenuation data, as in Duraiswami *et al.*⁷⁷ In line with the near resonance sound speed results, the attenuation data [Fig. 3(b)] shows that the present model predicts higher attenuation for single bubble sizes considered.

V. NONLINEAR SCATTERING

The scattering cross section may be defined in the long wavelength limit as the ratio of the total acoustic power scattered by an object at a given frequency to the incoming plane wave acoustic intensity I_0 :

$$\sigma_s = \frac{4\pi r^2 I_s}{I_0}, \quad (24)$$

where $I_0 = |P_A|^2 / 2\rho_s c_p$ and $I_s = |P_b|^2 / 2\rho_s c_p$. To calculate the nonlinear scattering, the pressure P_b radiated from a single bubble is obtained from⁵⁹

$$P_b(r, t) = \frac{\rho_s}{r} (2RR\ddot{R} + R^2\ddot{R}). \quad (25)$$

If linear pulsations of bubbles are considered, the above equations reduce to

$$\sigma_s = \frac{4\pi R_0^2}{(\omega^2/\omega_0^2 - 1)^2 + 4\beta_{\text{tot}}^2/\omega^2}. \quad (26)$$

Furthermore, applicable to both linear and nonlinear scattering, when a bubble distribution is present, the scattering cross section per unit volume is

$$\sigma_v = \frac{1}{4\pi} \int_0^\infty n_b(R_0) \sigma_s dR_0, \quad (27)$$

where $n_b(R_0)$ is the bubble number density (as defined in Sec. III A), which is typically expressed in terms of discrete radius bins, e.g., with 1 μm width. In practice, the limits of the integration are determined by the minimum and maximum detectable bubble size, which are deduced from the excitation frequency range through the use of Eq. (19). The volume backscattering strength (S_v) of a bubble population

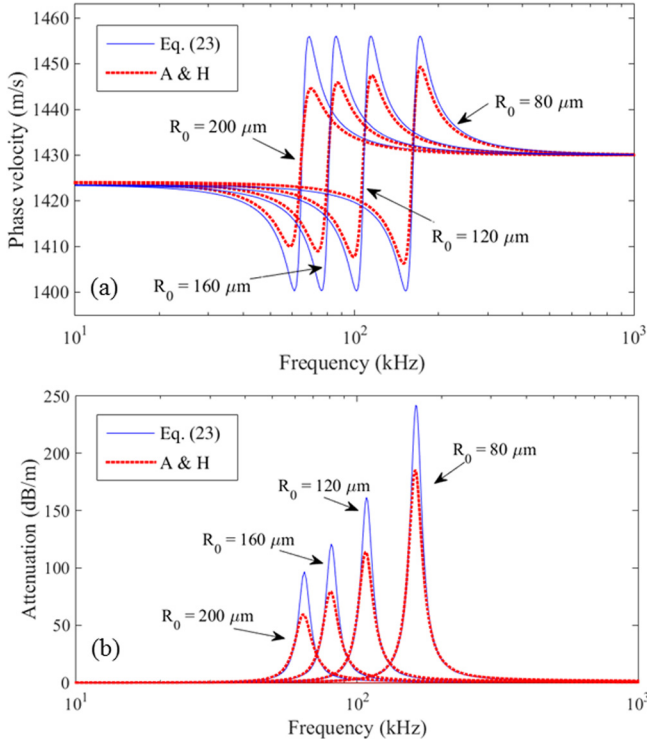


FIG. 3. (Color online) (a) Sound speed and (b) Attenuation as function of frequency for a series of monodisperse bubble populations, all having a void fraction of 10^{-5} (the bubble radius for each being labelled on the figure). The dashed line shows the predictions of the Anderson and Hampton model (Ref. 53) (A&H), and the solid line shows the results of the current formulation.

is defined with the reference volume cross section $\sigma_{v,ref} = 1 \text{ m}^2/\text{m}^3$:

$$S_v = 10 \log_{10}(\sigma_v/\sigma_{v,ref}). \quad (28)$$

The difference between the present model and Anderson and Hampton's theory is demonstrated by means of applying Eqs. (24)–(26), respectively. The results are shown in Fig. 4, the input bubble size distribution for the calculation being shown in the inset. The present model predicts lower values of the backscattering strength owing to the fundamental differences of the formulations. Although the steady-state responses are shown in Fig. 4, the current model is capable of modelling transient behaviour such as ring-up and ring-down periods during the insonification.

Note that the nonlinearity referred to in this section manifests itself in two distinct fashions. The first one is the nonlinear pulsations of gas bubbles as demonstrated above, and the second one is the nonlinear mixing of frequency components when dual frequency excitation techniques are employed. The majority of the studies which used dual frequency techniques derived analytical expressions for the scattered pressure spectral component at the difference-frequency, e.g., see Refs. 16, 17, 63, and 64. An alternative approach⁷⁸ suggests that the cumbersome scattering cross-section expressions encountered in dual frequency excitation can be avoided by numerically calculating the time history of the bubble radius Eq. (2), inserting these values into Eq. (25) to obtain the scattered pressure field, and applying a Fourier transform to determine the spectral components of the scattered pressure. The pressure spectral amplitudes are then compared to the recorded experimental data at each frequency, which yields the determination of the number of bubbles per unit volume. This numerical approach has been applied for bubble sizing in water tank experiments by Leighton *et al.*⁷⁸ and in sediments by Mantouka.⁷⁹

An example numerical computation of the spectral amplitude is shown in Fig. 5. The nonlinear volume backscattering strength at twice the insonification frequency is plotted vs the insonification frequency for the bubble

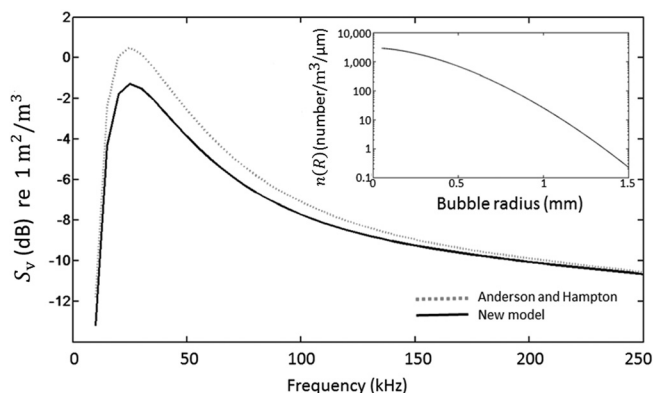


FIG. 4. Volume backscattering strength (defined with the reference volume cross section $\sigma_{v,ref} = 1 \text{ m}^2/\text{m}^3$) vs the frequency, corresponding to the bubble size distribution (BSD) shown in the inset. The scattering cross-section expressions are used according to the Anderson and Hampton formulation (dotted line) and the present model (solid line). The inset BSD has a void fraction of 2.26×10^{-4} .

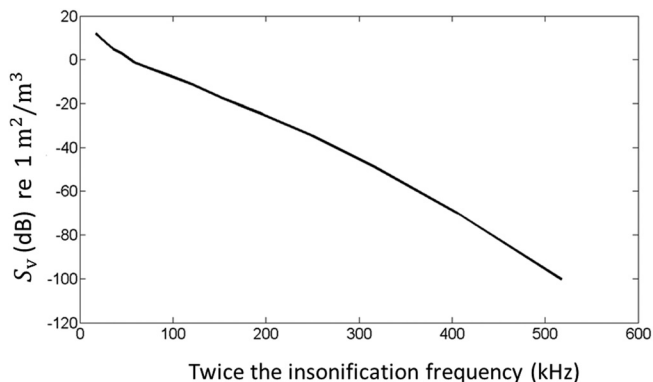


FIG. 5. The nonlinear volume backscattering strength at twice the insonification frequency (defined with the reference volume cross section $\sigma_{v,ref} = 1 \text{ m}^2/\text{m}^3$).

distribution shown in the inset of Fig. 4. First, R , \dot{R} , and \ddot{R} were computed from Eq. (2) assuming a monochromatic incident wave $P_A e^{i\omega t}$, and substituted into Eq. (25) to calculate the scattered pressure $P_b(t)$. The power spectra of the time series of P_b were calculated using a Fourier transform, and the spectral component nearest twice the insonification frequency is then used in Eq. (28) (using normalized values). Only bubbles resonant at the insonification frequency give strong nonlinear scattering at twice the frequency. Hence the beginning of the curve corresponds to the first frequency where the bubbles of $50 \mu\text{m}$ are resonant (which is the assumed small-bubble limit of the bubble distribution in the simulation).

VI. DISCUSSION AND CONCLUSIONS

This paper has presented a nonlinear model for gas bubble pulsations in marine sediments. The expressions are linearized to determine the resonance frequency and the damping terms for linear bubble pulsations, and then used to predict the effects that such bubble pulsations will have on the sound speed and attenuation of acoustic waves propagating in gassy marine sediment. The results between the current model and an existing theory (Anderson and Hampton) show significant differences at near resonance regimes. One major advantage of the present model is that, without user intervention to overcome the sign ambiguity, it can automatically produce objective prediction of sound speed and attenuation, and invert measurements of these parameters to infer the bubble population. Furthermore, the bubble pulsation model Eq. (2) can be used to predict the amplitudes of the scattered pressure field at the nonlinearly generated frequency components, i.e., the second harmonics, and combination and difference frequencies. Moreover, it can be included into a scheme to predict the effect on the sound speed and attenuation when the bubbles pulsate in a nonlinear manner (Leighton *et al.*⁵⁵). In this work, the formulation is proposed as a forward model and an improved alternative to the existing theory for gassy soft marine sediments. The inversion of real acoustic experimental data and the obtained bubble population results will be subject of a follow-up article.

As a preliminary analysis, the present formulation assumed the propagation of one compressional wave in the host medium (the far field pressure in existing theories is modelled with a single velocity potential without losses). Note that the work of Mantouka⁷⁹ heuristically accounted for the attenuation of the compressional wave, by assuming the forward model as in the present article but adding the corrections from the internal dissipation at the inversion stage (for bubble populations). A more comprehensive approach is required to incorporate the complex characteristics of the acoustic propagation in porous medium, i.e., the propagation of the second mode (slow wave), and the attenuation of the longitudinal modes due to internal dissipation, squirt flow and shear drag.⁸⁰ The addition of gas bubbles into the problem thereafter can be done by either modifying the radial dynamics Eq. (2) or extending the formulation in Kargl *et al.*⁴⁹

ACKNOWLEDGMENTS

This work is funded in part by the Natural Environment Research Council (NERC, RP008255) and the Engineering and Physical Sciences Research Council (EP/D000580/1; Principal Investigator: T.G.L.) and STEMM-CCS (funded from the European Union's Horizon 2020 research and innovation programme under grant agreement No. 654462). Agni Mantouka's Ph.D. studentship was supported by ISVR's Rayleigh Scholarship Scheme. The authors wish to thank Dr. Gary Heald, Dr. Angus Best, Dr. Paul Fox, and Dr. Justin Dix for useful discussions. H.D.'s contributions were supported by NERC (NE/J022403/1; Principal Investigator: T.G.L.). The data supporting this study are openly available from the University of Southampton repository at <http://dx.doi.org/10.5258/SOTON/397175>.

- ¹G. C. Sills and S. J. Wheeler, "The significance of gas for offshore operations," *Cont. Shelf Res.* **12**(10) 1239–1250 (1992).
- ²G. C. Sills, S. J. Wheeler, S. D. Thomas, and T. N. Gardiner, "Behaviour of offshore soils containing gas bubbles," *Geotechnique* **41**, 227–241 (1991).
- ³K. B. Briggs and M. D. Richardson, "Variability in *in situ* shear strength of gassy muds," *Geo-Mar. Lett.* **16**, 189–195 (1996).
- ⁴T. G. Leighton and P. R. White, "Quantification of undersea gas leaks from carbon capture and storage facilities, from pipelines and from methane seeps, by their acoustic emissions," *Proc. R. Soc. A* **468**, 485–510 (2012).
- ⁵E. J. Sauter, S. I. Muyakshin, J. L. Charlou, M. Schlüter, A. Boetius, K. Jerosch, E. Damm, J. P. Foucher, and M. Klages, "Methane discharge from a deep-sea submarine mud volcano into the upper water column by gas hydrate-coated methane bubbles," *Earth Planet. Sci. Lett.* **243**, 354–365 (2006).
- ⁶I. Leifer, D. Roberts, J. Margolis, and F. Kinnaman, "*In situ* sensing of methane emissions from natural marine hydrocarbon seeps: A potential remote sensing technology," *Earth Planet. Sci. Lett.* **245**, 509–522 (2006).
- ⁷A. I. Best, M. D. Richardson, B. P. Boudreau, A. G. Judd, I. Leifer, A. P. Lyons, C. S. Martens, D. L. Orange, and S. J. Wheeler, "Shallow bed methane gas could pose coastal hazard," *EOS Trans.* **87**(22), 213–217 (2006).
- ⁸J. Blackford, H. Stahl, J. M. Bull, B. J. P. Bergès, M. Cevatoglu, A. Lichtschlag, D. Connelly, R. H. James, J. Kita, D. Long, M. Naylor, K. Shitashima, D. Smith, P. Taylor, I. Wright, M. Akhurst, B. Chen, T. M. Gernon, C. Hauton, M. Hayashi, H. Kaieda, T. G. Leighton, T. Sato, M. D. J. Sayer, M. Suzumura, K. Tait, M. E. Vardy, P. R. White, and S. Widdicombe, "Detection and impacts of leakage from sub-seafloor deep geological carbon dioxide storage," *Nat. Clim. Change* **4**, 1011–1016 (2014).

- ⁹J. Blackford, J. M. Bull, M. Cevatoglu, D. Connelly, C. Hauton, R. H. James, A. Lichtschlag, H. Stahl, S. Widdicombe, and I. C. Wright, "Marine baseline and monitoring strategies for carbon dioxide capture and storage (CCS)," *Int. J. Greenhouse Gas Control* **38**, 221–229 (2015).
- ¹⁰B. J. P. Berges, T. G. Leighton, and P. R. White, "Passive acoustic quantification of gas fluxes during controlled gas release experiments," *Int. J. Greenhouse Gas Control* **38**, 64–79 (2015).
- ¹¹T. G. Leighton and G. Robb, "Preliminary mapping of void fractions and sound speeds in gassy marine sediments from subbottom profiles," *J. Acoust. Soc. Am.* **124**(5), EL313–EL320 (2008).
- ¹²G. B. N. Robb, S. P. Robinson, P. D. Theobald, G. Hayman, V. F. Humphrey, T. G. Leighton, L. S. Wang, J. K. Dix, and A. I. Best, "Absolute calibration of hydrophones immersed in sandy sediment," *J. Acoust. Soc. Am.* **125**(5), 2918–2927 (2009).
- ¹³T. G. Leighton, A. D. Phelps, D. G. Ramble, and D. A. Sharpe, "Comparison of the abilities of eight acoustic techniques to detect and size a single bubble," *Ultrasonics* **34**, 661–667 (1996).
- ¹⁴E. A. Zabolotskaya and S. I. Soluyan, "Emission of harmonic and combination frequency waves by air bubbles," *Sov. Phys. Acoust.* **18**, 396–398 (1973).
- ¹⁵T. G. Leighton, D. G. Ramble, and A. D. Phelps, "The detection of tethered and rising bubbles using multiple acoustic techniques," *J. Acoust. Soc. Am.* **101**, 2626–2635 (1997).
- ¹⁶S. V. Karpov, Z. Klusek, A. L. Matveev, A. I. Potapov, and A. M. Sutin, "Nonlinear interaction of acoustic wave in gas-saturated marine sediments," *Acoust. Phys.* **42**, 527–533 (1996).
- ¹⁷F. A. Boyle and N. P. Chotiros, "Nonlinear acoustic scattering from a gassy poroelastic seabed," *J. Acoust. Soc. Am.* **103**, 1328–1336 (1998).
- ¹⁸Z. Klusek, A. Sutin, A. Matveev, and A. Potapov, "Observation of nonlinear scattering of acoustical waves at sea sediments," *Acoust. Lett.* **18**, 198–203 (1995).
- ¹⁹T. G. Leighton, "The Rayleigh—Plesset equation in terms of volume with explicit shear losses," *Ultrasonics* **48**, 85–90 (2008).
- ²⁰T. G. Leighton, "Theory for acoustic propagation in marine sediment containing gas bubbles which may pulsate in a non-stationary nonlinear model," *Geophys. Res. Lett.* **34**, L17607, doi:10.1029/2007GL030803 (2007).
- ²¹E. L. Hamilton, "Compressional wave attenuation in marine sediments," *Geophysics* **37**, 620–646 (1972).
- ²²S. S. Fu, R. H. Wilkens, and L. N. Frazer, "*In situ* velocity profiles in gassy sediments: Kiel Bay," *Geo-Mar. Lett.* **16**, 249–253 (1996).
- ²³M. D. Richardson and K. B. Briggs, "*In situ* and laboratory geoaoustic measurements in soft mud and hard-packed sand sediments: Implications for high-frequency acoustic propagation and scattering," *Geo-Mar. Lett.* **16**, 196–203 (1996).
- ²⁴G. B. N. Robb, A. I. Best, J. K. Dix, J. M. Bull, T. G. Leighton, and P. R. White, "The frequency dependence of compressional wave velocity and attenuation coefficient of intertidal marine sediments," *J. Acoust. Soc. Am.* **120**, 2526–2537 (2006).
- ²⁵E. L. Hamilton, G. Shumway, H. W. Menard, and C. J. Shipke, "Acoustics and other physical properties of shallow-water sediments off San Diego," *J. Acoust. Soc. Am.* **28**, 1–15 (1956).
- ²⁶E. L. Hamilton, "Attenuation of shear waves in marine sediments," *J. Acoust. Soc. Am.* **60**, 334–338 (1976).
- ²⁷E. L. Hamilton and R. T. Bachman, "Sound velocity and related properties of marine sediments," *J. Acoust. Soc. Am.* **72**, 1891–1904 (1982).
- ²⁸G. Shumway, "Sound speed and absorption studies of marine sediment by a resonance method," *Geophysics* **25**, 451–467 (1960).
- ²⁹G. Shumway, "Sound speed and absorption studies of marine sediment by a resonance method—Part II," *Geophysics* **25**, 659–681 (1960).
- ³⁰A. I. Best, Q. J. Huggett, and A. J. K. Harris, "Comparison of *in situ* and laboratory acoustic measurements on Lough Hyne marine sediments," *J. Acoust. Soc. Am.* **110**, 695–709 (2001).
- ³¹M. D. Richardson, K. B. Briggs, L. D. Bibee, P. A. Jumars, W. B. Sawyer, D. B. Albert, R. H. Bennett, T. K. Berger, M. J. Buckingham, N. P. Chotiros, P. H. Dahl, N. T. Dewitt, P. Fleischer, R. Flood, C. F. Greenlaw, D. V. Holliday, and Hulbert, "Overview of SAX99: Environmental considerations," *IEEE J. Oceanic Eng.* **26**, 26–53 (2001).
- ³²J. Yang, D. Tang, and K. L. Williams, "Direct measurement of sediment sound speed in Shallow Water '06," *J. Acoust. Soc. Am.* **124**, EL116–EL121 (2008).
- ³³A. Turgut and T. Yamamoto, "Measurements of acoustic wave velocities and attenuations in marine sediment," *J. Acoust. Soc. Am.* **87**, 2376–2383 (1990).

- ³⁴G. Robb, A. Best, J. Dix, P. White, T. Leighton, J. Bull, and A. Harris, "The measurement of the *in situ* compressional wave properties of marine sediments," *IEEE J. Oceanic Eng.* **32**, 484–496 (2007).
- ³⁵A. B. Wood and D. E. Weston, "The propagation of sound in mud," *Acustica* **14**, 156–162 (1964).
- ³⁶F. A. Bowles, "Observations on attenuation and shear-wave velocity in fine-grained marine sediments," *J. Acoust. Soc. Am.* **101**, 3385–3397 (1997).
- ³⁷R. D. Stoll, "Experimental studies of attenuation in sediments," *J. Acoust. Soc. Am.* **66**(4), 1152–1160 (1979).
- ³⁸B. A. Brunson and R. K. Johnson, "Laboratory measurements of shear wave attenuation in saturated sand," *J. Acoust. Soc. Am.* **68**, 1371–1375 (1980).
- ³⁹M. A. Biot, "Theory of propagation of elastic waves in fluid-saturated porous solids: I. Low-frequency range," *J. Acoust. Soc. Am.* **28**(2), 168–178 (1956).
- ⁴⁰M. A. Biot, "Theory of propagation of elastic waves in fluid-saturated porous solids: II. Higher frequency range," *J. Acoust. Soc. Am.* **28**(2), 179–191 (1956).
- ⁴¹R. D. Stoll, "Marine sediment acoustics," *J. Acoust. Soc. Am.* **77**(5), 1789–1799 (1985).
- ⁴²J. G. Berryman, "Confirmation of Biot's theory," *Appl. Phys. Lett.* **37**(4), 382–384 (1980).
- ⁴³K. L. Williams, D. R. Jackson, E. I. Thorsos, and D. Tang, "Comparison of sound speed and attenuation measured in a sandy sediment to predictions based on the Biot theory of porous media," *IEEE J. Ocean. Eng.* **27**, 413–428 (2002).
- ⁴⁴D. R. Jackson and M. D. Richardson, *High-Frequency Seafloor Acoustics* (Springer, New York, 2007), pp. 1–616.
- ⁴⁵J. A. Hawkins and A. Bedford, "Variational theory of bubbly media with a distribution of bubble sizes. 2: Porous solids," *Int. J. Eng. Sci.* **30**(9), 1177–1186 (1992).
- ⁴⁶J. L. Buchanan, "A comparison of broadband models for sand sediments," *J. Acoust. Soc. Am.* **120**(6), 3584–3598 (2006).
- ⁴⁷D. M. J. Smeulders and M. E. H. Van Dongen, "Wave propagation in porous media containing a dilute gas-liquid mixture," *J. Fluid Mech.* **343**, 351–373 (1997).
- ⁴⁸A. L. Anderson, F. Abegg, J. A. Hawkins, M. E. Duncan, and A. P. Lyons, "Bubble populations and acoustic interaction with the gassy floor of Eckernforde Bay," *Cont. Shelf Res.* **18**, 1807–1838 (1998).
- ⁴⁹S. G. Kargl, K. L. Williams, and R. Lim, "Double monopole resonance of a gas-filled, spherical cavity in a sediment," *J. Acoust. Soc. Am.* **103**(1), 265–274 (1998).
- ⁵⁰F. A. Boyle and N. P. Chotiros, "A model for acoustic backscatter from muddy sediments," *J. Acoust. Soc. Am.* **98**(1), 525–530 (1995).
- ⁵¹F. A. Boyle and N. P. Chotiros, "A model for high-frequency acoustic backscatter from gas bubbles in sandy sediments at shallow grazing angles," *J. Acoust. Soc. Am.* **98**(1), 531–541 (1995).
- ⁵²A. L. Anderson and L. D. Hampton, "Acoustics of gas-bearing sediments. I. Background," *J. Acoust. Soc. Am.* **67**(6), 1865–1889 (1980).
- ⁵³A. L. Anderson and L. D. Hampton, "Acoustics of gas-bearing sediment. II. Measurements and models," *J. Acoust. Soc. Am.* **67**(6), 1890–1903 (1980).
- ⁵⁴A. I. Best, M. D. J. Tuffin, J. K. Dix, and J. M. Bull, "Tidal height and frequency dependence of acoustic velocity and attenuation in shallow gassy marine sediments," *J. Geophys. Res. B* **109**, 08101, doi:10.1029/2003JB002748 (2004).
- ⁵⁵T. G. Leighton, S. D. Meers, and P. R. White, "Propagation through nonlinear time-dependent bubble clouds and the estimation of bubble populations from measured acoustic characteristics," *Proc. R. Soc. London Ser. A* **460**(2049), 2521–2550 (2004).
- ⁵⁶A. P. Lyons, M. E. Duncan, and A. L. Anderson, "Predictions of the acoustic scattering response of free-methane bubbles in muddy sediments," *J. Acoust. Soc. Am.* **99**(1), 163–172 (1996).
- ⁵⁷M. A. Ainslie and T. G. Leighton, "Near resonant bubble acoustic cross-section corrections, including examples from oceanography, volcanology, and biomedical ultrasound," *J. Acoust. Soc. Am.* **126**(5), 2163–2175 (2009).
- ⁵⁸M. A. Ainslie and T. G. Leighton, "Review of scattering and extinction cross-sections, damping factors, and resonance frequencies of a spherical gas bubble," *J. Acoust. Soc. Am.* **130**(5), 3184–3208 (2011).
- ⁵⁹J. W. L. Clarke and T. G. Leighton, "A method for estimating time-dependent acoustic cross-sections of bubbles and bubble clouds prior to the steady state," *J. Acoust. Soc. Am.* **107**(4), 1922–1929 (2000).
- ⁶⁰A. D. Phelps, D. G. Ramble, and T. G. Leighton, "The use of a combination frequency technique to measure the surf zone bubble population," *J. Acoust. Soc. Am.* **101**(4), 1981–1989 (1997).
- ⁶¹A. D. Phelps and T. G. Leighton, "Oceanic bubble population measurements using a buoy-deployed combination frequency technique," *IEEE J. Oceanic Eng.* **23**, 400–410 (1998).
- ⁶²T. G. Leighton, R. J. Lingard, A. J. Walton, and J. E. Field, "Acoustic bubble sizing by the combination of subharmonic emissions with an imaging frequency," *Ultrasonics* **29**, 319–323 (1991).
- ⁶³L. A. Ostrovsky, A. M. Sutin, I. A. Soustova, A. L. Matveyev, A. I. Potapov, and Z. Kluzek, "Nonlinear scattering of acoustic waves by natural and artificially generated subsurface bubble layers in sea," *J. Acoust. Soc. Am.* **113**(2), 741–749 (2003).
- ⁶⁴A. M. Sutin, S. W. Yoon, E. J. Kim, and I. N. Didenkulov, "Nonlinear acoustic method for bubble density measurements in water," *J. Acoust. Soc. Am.* **103**(5), 2377–2384 (1998).
- ⁶⁵J. G. Berryman, "Long-wavelength propagation in composite elastic media. I. Spherical inclusions," *J. Acoust. Soc. Am.* **68**(6), 1808–1819 (1980).
- ⁶⁶J. G. Berryman, "Long-wavelength propagation in composite elastic media. II. Ellipsoidal inclusions," *J. Acoust. Soc. Am.* **68**(6), 1820–1831 (1980).
- ⁶⁷X. Yang and C. C. Church, "A model for dynamics of gas bubbles in soft tissue," *J. Acoust. Soc. Am.* **118**(6), 3595–3606 (2005).
- ⁶⁸A. Prosperetti, L. Crum, and K. Commander, "Nonlinear bubble dynamics," *J. Acoust. Soc. Am.* **83**, 502–514 (1988).
- ⁶⁹J. P. Y. Maa and A. J. Mehta, "Soft mud properties: Voigt model," *J. Waterw., Port, Coastal, Ocean Eng.* **114**(6), 765–770 (1988).
- ⁷⁰H. Macpherson, "The attenuation of water waves over a non-rigid bed," *J. Fluid Mech.* **97**(4), 721–742 (1980).
- ⁷¹H. T. Chou, M. A. Foda, and J. R. Hunt, "Rheological response of cohesive sediments to oscillatory forcing," in *Nearshore and Estuarine Cohesive Sediment Transport, Coastal Estuarine Sci. Ser.* (AGU Washington, DC, 2013), Vol. 42, pp. 126–147.
- ⁷²M. A. Foda, J. R. Hunt, and H. T. Chou, "A nonlinear model for the fluidization of marine muds by waves," *J. Geophys. Res.* **98**(C4), 7039–7047, doi:10.1029/92JC02797 (1993).
- ⁷³M. Jain and A. J. Mehta, "Role of basic rheological models in determination of wave attenuation over muddy seabeds," *Cont. Shelf Res.* **29**, 642–651 (2009).
- ⁷⁴K. W. Commander and A. Prosperetti, "Linear pressure waves in bubbly liquids: Comparison between theory and experiment," *J. Acoust. Soc. Am.* **85**, 732–746 (1989).
- ⁷⁵G. E. Claypool and I. R. Kaplan, "The origin and distribution of methane in marine sediments," in *Natural Gases in Marine Sediments* (Plenum, New York, 1974), pp. 99–139.
- ⁷⁶G. Mavko, T. Mukerij, and J. Dvorkin, *The Rock Physics Handbook* (Cambridge University Press, Cambridge, UK, 1998), pp. 1–511.
- ⁷⁷R. Duraiswami, S. Prabhukumar, and G. L. Chahine, "Bubble counting using an inverse acoustic scattering method," *J. Acoust. Soc. Am.* **104**, 2699–2717 (1998).
- ⁷⁸T. G. Leighton, A. Mantouka, P. R. White, and Z. Klusek, "Towards field measurements of populations of methane gas bubbles in marine sediment: An inversion method required for interpreting two-frequency insonification data from sediment containing gas bubbles," *Hydroacoustics* **11**, 203–224 (2008).
- ⁷⁹A. Mantouka, "Development of a two-frequency technique for gas-bubble sizing in marine sediment," Ph.D. thesis, University of Southampton, 2010.
- ⁸⁰N. P. Chotiros and M. J. Isakson, "A broadband model of sandy ocean sediments: Biot—Stoll with contact squirt flow and shear drag," *J. Acoust. Soc. Am.* **116**(4), 2011–2022 (2004).